III. Theory of Optical Delay Line Coupling Quantum Neural Network

In this Chapter, we present the quantum theory of degenerate optical parametric oscillator (DOPO) networks based on optical delay line coupling, which have been recently demonstrated at Stanford, NII and NTT [1–3]. Two types of c-number stochastic differential equations (CSDE) are derived using the (exact) positive $P(\alpha, \beta)$ representation [4] and the (approximate) truncated Wigner representation of the density operator [5]. We introduce the EPR-like operator and the quantum discord to evaluate the quantum noise correlation and entanglement formed in the DOPOs during the computation process.

3.1 Standard theoretical approach and computational difficulty

Figure 1(a) shows a schematic illustration of the simplest model of two coupled DOPOs considered in this Chapter. The system is composed of two DOPO cavities and a mutual injection path between them. The coherent pump field ε_p enters each DOPO cavity to excite the intra-cavity pump mode. The bosonic annihilation and creation operators for the pump and signal modes in the DOPOs are denoted as $(\hat{a}_{pj}, \hat{a}_{pj}^\dagger)$ and $(\hat{a}_{sj}, \hat{a}_{sj}^\dagger)$, where j $(= 1, 2)$ is the index for the DOPO. Also, the creation and annihilation operators for the signal mode in the mutual injection path are written as $(\hat{a}_c, \hat{a}_c^\dagger)$. Figure 1(b) displays the coupling between the DOPO intra-cavity signal fields and the injection path signal field, which is described as beam splitter interactions. Here, the signal field in the injection path interacts with the two DOPO intra-cavity fields at distant points, thus we have to consider the spatial phase explicitly. The phase factors for the bosonic operators at the facet of the DOPO#2 depend on the injection path length z and are written as $\hat{a}_c \exp(ik_c z)$ and $\hat{a}_c^\dagger \exp(-ik_c z)$, where k_c is the wave number for the signal mode in the injection path. The mutual couplings are in-phase (ferromagnetic) if $\exp(ik_c z) = \exp(-ik_c z) = 1$, and out of phase (anti-ferromagnetic) if $\exp(ik_c z) = \exp(-ik_c z) = -1$.

The Hamiltonian for the total system can be written as

$$\hat{\mathcal{H}} = \hat{\mathcal{H}}_{\text{free}} + \hat{\mathcal{H}}_{\text{int}} + \hat{\mathcal{H}}_{\text{pump}} + \hat{\mathcal{H}}_{\text{res}} + \hat{\mathcal{H}}_{\text{BS}}, \tag{1}$$

where the free Hamiltonian for the relevant modes is

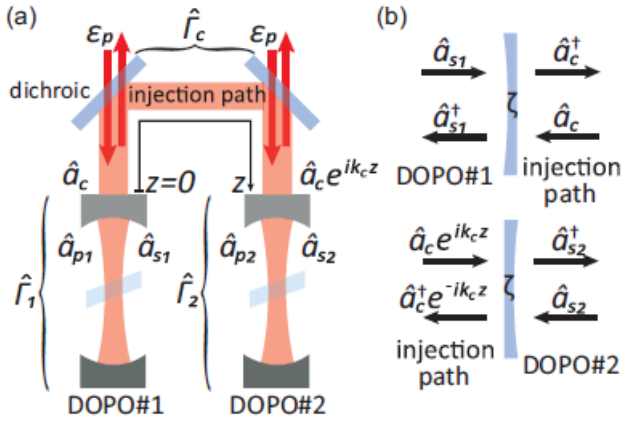

FIG. 1: (Color online) Schematic of the simplest model for optical delay line coupling QNN. (a) The system comprises two DOPOs and a mutual injection path between them as a cavity. The two dichroic mirrors in the injection path are assumed to pass the pump field completely and highly reflect the signal field. (b) Beam splitter interactions between the DOPO intra-cavity signal fields and the injection-path mode. The spatial phase of the injection-path field should be considered [4].

$$\hat{\mathcal{H}}_{\text{free}} = \sum_{j=1}^{2} \left(\hbar\omega_p \hat{a}_{pj}^\dagger \hat{a}_{pj} + \hbar\omega_s \hat{a}_{sj}^\dagger \hat{a}_{sj} \right) + \hbar\omega_s \hat{a}_c^\dagger \hat{a}_c, \tag{2}$$

where ω_s is the frequency of the signal field and $\omega_p = 2\omega_s$. The parametric interaction Hamiltonian is

$$\hat{\mathcal{H}}_{\text{int}} = i\hbar \sum_{j=1}^{2} \left[\frac{\kappa}{2} \left(\hat{a}_{sj}^{\dagger 2} \hat{a}_{pj} - \hat{a}_{pj}^\dagger \hat{a}_{sj}^2 \right) \right], \tag{3}$$

where κ denotes the parametric coupling coefficient (see Chapter II) . The pumping Hamiltonian is described by

$$\hat{\mathcal{H}}_{\text{pump}} = i\hbar \sum_{j=1}^{2} \left[\varepsilon_p \hat{a}_{pj}^\dagger \exp\left(-i\omega_d t\right) - \varepsilon_p \hat{a}_{pj} \exp\left(i\omega_d t\right) \right], \tag{4}$$

where the pump field ε_p is set to be positive and real, and ω_d is the frequency of the external pump field ε_p with $\omega_d \approx \omega_p$. The beam splitter coupling constant between external and internal pump fields is absorbed in ε_p. The system-reservoir coupling Hamiltonian for the signal, pump and injection path modes is written as

$$\hat{\mathcal{H}}_{\text{res}} = \hbar \sum_{j=1}^{2} \left(\hat{a}_{sj} \hat{\Gamma}_{Rsj}^\dagger + \hat{\Gamma}_{Rsj} \hat{a}_{sj}^\dagger + \hat{a}_{pj} \hat{\Gamma}_{Rpj} + \hat{\Gamma}_{Rpj} \hat{a}_{pj}^\dagger \right) + \left(\hat{a}_c \hat{\Gamma}_{Rc}^\dagger + \hat{\Gamma}_{Rc} \hat{a}_c^\dagger \right), \tag{5}$$

where $\hat{\Gamma}_{Rsj}, \hat{\Gamma}_{Rpj}$, and $\hat{\Gamma}_{Rc}$ are the reservoir operators for the DOPO signal modes, pump modes, and injection path mode. Those reservoir operators have continuous and white spectra in frequency and thus induce the Fermi's golden rule decay rates, but the frequency mode indices are suppressed in Eq.(5) for simplicity. Finally, the beam splitter interaction Hamiltonian between the injection path mode and DOPO intra-cavity signal modes is denoted by

$$\hat{\mathcal{H}}_{\mathrm{BS}} = i\hbar\zeta \left(\hat{a}_c \hat{a}_{s1}^{\dagger} - \hat{a}_c^{\dagger} \hat{a}_{s1} + \hat{a}_{s2} \hat{a}_c^{\dagger} e^{-ik_c z} - \hat{a}_{s2}^{\dagger} a e^{ik_c z} \right), \tag{6}$$

where ζ is the beam splitter coupling coefficient.

Using the standard quantum optics technique [6], we can derive the master equation for the total density operator consisting of the two intra-cavity signal fields, two intra-cavity pump fields and one injection path signal field. If we expand the density operator by the photon number eigenstates, $|n_{s1}, n_{s2}, n_{p1}, n_{p2}, n_c\rangle$, which form an orthonormal set for the total system, the dimension of the density matrix is too large to compute its time evolution numerically, since the upper bound of the photon number is much larger than one for each mode. When the QNN consists of $N(\gg 1)$ DOPOs instead of two DOPOs, the exponential increase in the Hilbert space makes a numerical study even more intractable.

3.2 Positive $P(\alpha, \beta)$ representation

A coherent state $|\alpha\rangle$, which is an eigenstate of the annihilation operator [7], provides an ideal basis set for expanding the field density operator for such a system. The primary reason for the preferred choice of coherent states is that the initial states and the final states of the signal, pump and injection path fields are close to coherent states. The secondary reason is that a coherent state remains a coherent state when the field is dissipated by linear optical losses if the reservoir temperature can be assumed to be zero, which is obviously true in our case.

We now introduce the positive P representation [8] for the five modes to expand the total density operator:

$$\hat{\rho} = \int P(\alpha, \beta) \frac{|\alpha\rangle\langle\beta^*|}{\langle\beta^*|\alpha\rangle} \mathrm{d}\alpha \mathrm{d}\beta. \tag{7}$$

Here, $\alpha = (\alpha_{s1}, \alpha_{s2}, \alpha_{p1}, \alpha_{p2}, \alpha_c)^T$ and $\beta = (\beta_{s1}, \beta_{s2}, \beta_{p1}, \beta_{p2}, \beta_c)^T$ contain ten c-number variables to describe the multimode coherent states $|\alpha\rangle = |\alpha_{s1}\rangle |\alpha_{s2}\rangle |\alpha_{p1}\rangle |\alpha_{p2}\rangle |\alpha_c\rangle$ and $\langle\beta^*| = \langle\beta_c^*| \langle\beta_{p2}^*| \langle\beta_{p1}^*| \langle\beta_{s2}^*| \langle\beta_{s1}^*|$. These product states are used as a basis set for expanding the density operator. The positive $P(\alpha, \beta)$ representation gives a positive and appropriately normalized distribution function, where α_X and β_X undergo statistically independent random processes in probabilistic simulations while they are complex conjugate in average, i.e., $\langle\alpha_X\rangle = \langle\beta_X\rangle^*$. Here, X is the index for specifying the five modes.

We substitute Eq.(7) into the master equation and obtain the Fokker-Planck equation (FPE) for the distribution $P(\alpha, \beta)$ [4]:

$$\begin{aligned}
\frac{\partial}{\partial t}P(\alpha,\beta) = & \Bigg\{ \sum_{j=1}^{2} \Bigg[\frac{\partial}{\partial \alpha_{sj}} \Big((\gamma_s + i\Delta_s)\alpha_{sj} - \kappa\beta_{sj}\alpha_{pj} \Big) \\
& + \frac{\partial}{\partial \beta_{sj}} \Big((\gamma_s - i\Delta_s)\beta_{sj} - \kappa\alpha_{sj}\beta_{pj} \Big) \\
& + \frac{\partial}{\partial \alpha_{pj}} \Big((\gamma_p + i\Delta_p)\alpha_{pj} - \varepsilon_p + \frac{\kappa^2}{2}\alpha_{sj}^2 \Big) \\
& + \frac{\partial}{\partial \beta_{pj}} \Big((\gamma_p - i\Delta_p)\beta_{pj} - \varepsilon_p + \frac{\kappa^2}{2}\beta_{sj}^2 \Big) \\
& + \frac{1}{2} \Big(\frac{\partial^2}{\partial \alpha_{pj}^2}\kappa\alpha_{pj} + \frac{\partial^2}{\partial \beta_{pj}^2}\kappa\beta_{pj} + \frac{\partial^2}{\partial \alpha_{sj}\partial \beta_{sj}}\Gamma_{sj} + \frac{\partial^2}{\partial \alpha_{pj}\partial \beta_{pj}}\Gamma_{pj} \Big) \Bigg] \\
& + \Bigg[\frac{\partial}{\partial \alpha_c}(\gamma_c + i\Delta_s)\alpha_c + \frac{\partial}{\partial \beta_c}(\gamma_c + i\Delta_s)\beta_c + \frac{1}{2}\frac{\partial^2}{\partial \alpha_c \partial \beta_c}\Gamma_c \\
& - \frac{\partial}{\partial \alpha_{s1}}\zeta\alpha_c - \frac{\partial}{\partial \beta_{s1}}\zeta\beta_c + \frac{\partial}{\partial \alpha_{s2}}\zeta\alpha_c e^{i\theta} + \frac{\partial}{\partial \beta_{s2}}\zeta\beta_c e^{-i\theta} \\
& + \frac{\partial}{\partial \alpha_c}\zeta\left(\alpha_{s1} - \alpha_{s2}e^{-i\theta}\right) + \frac{\partial}{\partial \beta_c}\zeta\left(\beta_{s1} - \beta_{s2}e^{i\theta}\right) \Bigg] \Bigg\} P(\boldsymbol{\alpha}, \boldsymbol{\beta}),
\end{aligned} \tag{8}$$

where $\theta = k_c z$ is the injection path phase shift. $\Delta_s = \omega_s - \omega_d/2$ and $\Delta_p = \omega_p - \omega_d$ are the detuning between the intra-cavity modes and the external driving field ε_p.

With the Ito's rule [9], which establishes the correspondence between the FPEs and CSDEs, we reach a series of Ito-type CSDEs [4]:

$$
\mathrm{d}\begin{bmatrix}\alpha_{s1}\\ \beta_{s1}\end{bmatrix} = \begin{bmatrix} -\left(\gamma_s + i\Delta_s\right)\alpha_{s1} + \kappa\beta_{s1}\alpha_{p1} - \zeta\alpha_c \\ -\left(\gamma_s - i\Delta_s\right)\beta_{s1} + \kappa\alpha_{s1}\beta_{p1} - \zeta\beta_c \end{bmatrix}\mathrm{d}t + \begin{bmatrix} \kappa\alpha_{p1} & \Gamma_s \\ \Gamma_s & \kappa\beta_{p1}\end{bmatrix}^{1/2}\begin{bmatrix}\mathrm{d}W_{\alpha s1}(t)\\ \mathrm{d}W_{\beta s1}(t)\end{bmatrix}, \tag{9}
$$

$$
\mathrm{d}\begin{bmatrix}\alpha_{s2}\\ \beta_{s2}\end{bmatrix} = \begin{bmatrix} -\left(\gamma_s + i\Delta_s\right)\alpha_{s2} + \kappa\beta_{s2}\alpha_{p2} + \zeta\alpha_c e^{i\theta} \\ -\left(\gamma_s - i\Delta_s\right)\beta_{s2} + \kappa\alpha_{s2}\beta_{p2} + \zeta\beta_c e^{-i\theta} \end{bmatrix}\mathrm{d}t + \begin{bmatrix} \kappa\alpha_{p2} & \Gamma_s \\ \Gamma_s & \kappa\beta_{p2}\end{bmatrix}^{1/2}\begin{bmatrix}\mathrm{d}W_{\alpha s2}(t)\\ \mathrm{d}W_{\beta s2}(t)\end{bmatrix}, \tag{10}
$$

$$
\mathrm{d}\begin{bmatrix}\alpha_{p1}\\ \beta_{p1}\end{bmatrix} = \begin{bmatrix} \varepsilon_p - \left(\gamma_p + i\Delta_p\right)\alpha_{p1} - \frac{\kappa}{2}\alpha_{s1}^2 \\ \varepsilon_p - \left(\gamma_p - i\Delta_p\right)\beta_{p1} - \frac{\kappa}{2}\beta_{s1}^2 \end{bmatrix}\mathrm{d}t + \begin{bmatrix} 0 & \Gamma_p \\ \Gamma_p & 0\end{bmatrix}^{1/2}\begin{bmatrix}\mathrm{d}W_{\alpha p1}(t)\\ \mathrm{d}W_{\beta p1}(t)\end{bmatrix}, \tag{11}
$$

$$
\mathrm{d}\begin{bmatrix}\alpha_{p2}\\ \beta_{p2}\end{bmatrix} = \begin{bmatrix} \varepsilon_p - \left(\gamma_p + i\Delta_p\right)\alpha_{p2} - \frac{\kappa}{2}\alpha_{s2}^2 \\ \varepsilon_p - \left(\gamma_p - i\Delta_p\right)\beta_{p2} - \frac{\kappa}{2}\beta_{s2}^2 \end{bmatrix}\mathrm{d}t + \begin{bmatrix} 0 & \Gamma_p \\ \Gamma_p & 0\end{bmatrix}^{1/2}\begin{bmatrix}\mathrm{d}W_{\alpha p2}(t)\\ \mathrm{d}W_{\beta p2}(t)\end{bmatrix}, \tag{12}
$$

$$
\mathrm{d}\begin{bmatrix}\alpha_{c}\\ \beta_{c}\end{bmatrix} = \begin{bmatrix} -\left(\gamma_c + i\Delta_s\right)\alpha_c - \zeta\alpha_{s1} + \zeta\alpha_{s2}e^{i\theta} \\ -\left(\gamma_c - i\Delta_s\right)\beta_c - \zeta\beta_{s1} + \zeta\beta_{s2}e^{-i\theta} \end{bmatrix}\mathrm{d}t + \begin{bmatrix} 0 & \Gamma_c \\ \Gamma_c & 0\end{bmatrix}^{1/2}\begin{bmatrix}\mathrm{d}W_{\alpha c}(t)\\ \mathrm{d}W_{\beta c}(t)\end{bmatrix}, \tag{13}
$$

where $\mathrm{d}W_X(t)$ is the real number Wiener increment statistically independent of each other. This term corresponds to the noise term in the equivalent (classical) Langevin equation whose autocorrelation is given as a delta function. However, note that $\mathrm{d}W_X$ does not include the vacuum fluctuation introduced by the dissipative loss to external reservoirs. The vacuum fluctuation is already included in the coherent state basis sets.

In the case of a resonant pumping $\Delta_s = \Delta_p = 0$ and zero temperature reservoirs $\Gamma_s =$

$\Gamma_p = \Gamma_c = 0$, we adiabatically eliminate the pump variables using the assumption that the pump fields decay sufficiently faster than the signal fields. Then we have a simplified model as follows [4]:

$$\begin{aligned} \mathrm{d}\alpha_{s1} =& \Big[-\gamma_s\alpha_{s1} + \frac{\kappa}{\gamma_p}\Big(\varepsilon_p - \frac{\kappa}{2}\alpha_{s1}^2\Big)\beta_{s1} + \zeta\alpha_c \Big]\mathrm{d}t \\ &+ \sqrt{\frac{\kappa}{\gamma_p}\Big(\varepsilon_p - \frac{\kappa}{2}\alpha_{s1}^2\Big)}\,\mathrm{d}W_{\alpha s1}(t), \end{aligned} \tag{14}$$

$$\begin{aligned} \mathrm{d}\beta_{s1} =& \Big[-\gamma_s\beta_{s1} + \frac{\kappa}{\gamma_p}\Big(\varepsilon_p - \frac{\kappa}{2}\beta_{s1}^2\Big)\alpha_{s1} + \zeta\beta_c \Big]\mathrm{d}t \\ &+ \sqrt{\frac{\kappa}{\gamma_p}\Big(\varepsilon_p - \frac{\kappa}{2}\beta_{s1}^2\Big)}\,\mathrm{d}W_{\beta s1}(t), \end{aligned} \tag{15}$$

$$\begin{aligned} \mathrm{d}\alpha_{s2} =& \Big[-\gamma_s\alpha_{s2} + \frac{\kappa}{\gamma_p}\Big(\varepsilon_p - \frac{\kappa}{2}\alpha_{s2}^2\Big)\beta_{s2} - \zeta\alpha_c e^{i\theta} \Big]\mathrm{d}t \\ &+ \sqrt{\frac{\kappa}{\gamma_p}\Big(\varepsilon_p - \frac{\kappa}{2}\alpha_{s2}^2\Big)}\,\mathrm{d}W_{\alpha s2}(t), \end{aligned} \tag{16}$$

$$\begin{aligned} \mathrm{d}\beta_{s2} =& \Big[-\gamma_\mathrm{s}\beta_{\mathrm{s}2} + \frac{\kappa}{\gamma_\mathrm{p}}\Big(\varepsilon_\mathrm{p} - \frac{\kappa}{2}\beta_{\mathrm{s}2}^2\Big)\alpha_{\mathrm{s}2} - \zeta\beta_\mathrm{c}\mathrm{e}^{-\mathrm{i}\theta} \Big]\mathrm{d}t \\ &+ \sqrt{\frac{\kappa}{\gamma_p}\Big(\varepsilon_p - \frac{\kappa}{2}\beta_{s2}^2\Big)}\,\mathrm{d}W_{\beta s2}(t), \end{aligned} \tag{17}$$

$$\mathrm{d}\alpha_c = \left(-\gamma_c\alpha_c - \zeta\alpha_{s1} + \zeta\alpha_{s2}e^{i\theta}\right)\mathrm{d}t, \tag{18}$$

$$\mathrm{d}\beta_c = \left(-\gamma_c\beta_c - \zeta\beta_{s1} + \zeta\beta_{s2}e^{-i\theta}\right)\mathrm{d}t. \tag{19}$$

We further consider the limit where the injection path mode decays faster than the DOPO intra-cavity signal fields, so that it is also adiabatically eliminated, i.e., $\gamma_c \gg \gamma_s$. The field in the injection path at the steady state is given by

$$\alpha_c = \frac{1}{\gamma_c}\left(-\zeta\alpha_{s1} + e^{i\theta}\zeta\alpha_{s2}\right), \tag{20}$$

$$\beta_c = \frac{1}{\gamma_c}\left(-\zeta\beta_{s1} + e^{-i\theta}\zeta\beta_{s2}\right). \tag{21}$$

Substituting Eqs.(20) and (21) into (14) - (19), we have the CSDEs for the DOPO signal fields. When we further define the effective signal loss γ_s' and the normalized beam splitter

coupling ξ as

$$\gamma'_s = \gamma_s + \frac{\zeta^2}{\gamma_c}, \quad \xi = \frac{\zeta^2}{\gamma_s\gamma_c + \zeta^2}, \tag{22}$$

then we have the normalized CSDEs for the signal modes as

$$\mathrm{d}\eta_j = \left[-\eta_j + \mu_j\left(p - \eta_j^2\right) + \xi\eta_k e^{i\theta}\right]\mathrm{d}\tau + g\sqrt{p - \eta_j^2}\,\mathrm{d}W_{\eta j}(\tau), \tag{23}$$

$$\mathrm{d}\mu_j = \left[-\mu_j + \eta_j\left(p - \mu_j^2\right) + \xi\mu_k e^{-i\theta}\right]\mathrm{d}\tau + g\sqrt{p - \mu_j^2}\,\mathrm{d}W_{\mu_j}(\tau). \tag{24}$$

Here, $\eta_j = g\alpha_{sj}$, $\mu_j = g\beta_{sj}$, and $g = \kappa/\sqrt{2\gamma'_s\gamma_p} = 1/2A_s$ is the saturation parameter, $p = \varepsilon_p/\varepsilon_{th}$ is the normalized pumping rate and $\varepsilon_{th} = \gamma'_s\gamma_p/\kappa$ is the pump rate at the oscillation threshold. The time is scaled with the signal field lifetime, i.e. $\tau = \gamma'_s t$. $\mathrm{d}W_{\eta j}(\tau)$ and $\mathrm{d}W_{\mu_j}(\tau)$ are rescaled Wiener increments. The linear mutual injection terms have an explicit coupling form $\xi\eta_k e^{i\theta}$ and $\xi\mu_k e^{-i\theta}$.

For high-Q DOPO cavities, we can expect $\zeta > \gamma_s$, and this is an important condition for the system to show such nontrivial quantum effects, as a Schrödinger's cat state and negative Wigner function (see Chapter V). The saturation parameter $g = \kappa/\sqrt{2\gamma'_s\gamma_p}$ determines the typical order of the photon number inside the DOPO cavity above the oscillation threshold, i.e., $\langle n_s\rangle \sim 1/g^2$ at above the threshold.

3.3 Truncated Wigner representation $W(\alpha)$

Alternatively, we can expand the total density operator ρ by the Wigner function $W(\alpha)$:

$$\rho = \int e^{\boldsymbol{\lambda}^*\hat{\boldsymbol{a}} - \boldsymbol{\lambda}\hat{\boldsymbol{a}}^\dagger}\left\{\int e^{\boldsymbol{\lambda}\boldsymbol{\alpha}^* - \boldsymbol{\lambda}^*\boldsymbol{\alpha}}W(\boldsymbol{\alpha})\mathrm{d}\boldsymbol{\alpha}\right\}\mathrm{d}\boldsymbol{\lambda}, \tag{25}$$

where $\hat{\boldsymbol{a}} = (\hat{a}_{s1}, \hat{a}_{s2}, \hat{a}_{p1}, \hat{a}_{p2}, \hat{a}_c)^{\mathrm{T}}$ and $\boldsymbol{\lambda} = (\lambda_{s1}, \lambda_{s2}, \lambda_{p1}, \lambda_{p2}, \lambda_c)$. $\boldsymbol{\alpha}$ and $\boldsymbol{\lambda}$ form a pair of complex numbers. $\chi(\boldsymbol{\lambda}) = \int e^{\boldsymbol{\lambda}\boldsymbol{\alpha}^* - \boldsymbol{\lambda}^*\boldsymbol{\alpha}}W(\boldsymbol{\alpha})\,\mathrm{d}\boldsymbol{\alpha}$ is the symmetric correlation function [9]. We substitute Eq.(25) into the master equation and the resulting Fokker-Planck equation, with the third and higher-order terms truncated, results in another set of CSDEs [5]:

$$
\begin{aligned}
\mathrm{d}\alpha_{s1} &= (-\gamma_s\alpha_{s1} + \kappa\alpha_{p1}\alpha_{s1}^* + \zeta\alpha_c)\mathrm{d}t + \sqrt{\gamma_s}\mathrm{d}W_{s1}(t) \\
\mathrm{d}\alpha_{s2} &= (-\gamma_s\alpha_{s2} + \kappa\alpha_{p2}\alpha_{s2}^* - \zeta e^{-ik_c z}\alpha_c)\mathrm{d}t + \sqrt{\gamma_s}\mathrm{d}W_{s2}(t) \\
\mathrm{d}\alpha_{p1} &= (-\gamma_p\alpha_{p1} - \tfrac{\kappa}{2}\alpha_{s1}^2 + \epsilon_p)\mathrm{d}t + \sqrt{\gamma_p}\mathrm{d}W_{p1}(t) \\
\mathrm{d}\alpha_{p2} &= (-\gamma_p\alpha_{p2} - \tfrac{\kappa}{2}\alpha_{s2}^2 + \epsilon_p)\mathrm{d}t + \sqrt{\gamma_p}\mathrm{d}W_{p2}(t) \\
\mathrm{d}\alpha_c &= (-\gamma_c\alpha_c - \zeta\alpha_{s1} + \zeta e^{ik_c z}\alpha_{s2})\mathrm{d}t + \sqrt{\gamma_c}\mathrm{d}W_c(t).
\end{aligned}
\tag{26}
$$

Here, $\mathrm{d}W_X(t)$ is the c-number Wiener process and expresses the vacuum and thermal noise injection associated with the dissipation of the signal, pump and injection path fields to external reservoirs. Next, we assume $\gamma_p, \gamma_c \gg \gamma_s$ and adiabatically eliminate the pump and injection path modes ($\mathrm{d}\alpha_{pj} = \mathrm{d}\alpha_c = 0$). We also assume $e^{ik_c z} = e^{-ik_c z} = -1$ (anti-ferromagnetic coupling). Finally, we obtain the CSDE for the normalized signal amplitude [5]:

$$
\begin{aligned}
\mathrm{d}A_{s1} &= \left\{-A_{s1} + (p - A_{s1}^2)A_{s1}^* - \xi A_{s2}\right\}\mathrm{d}\tau + g\mathrm{d}W'_{s1} \\
\mathrm{d}A_{s2} &= \left\{-A_{s2} + (p - A_{s2}^2)A_{s2}^* - \xi A_{s1}\right\}\mathrm{d}\tau + g\mathrm{d}W'_{s2},
\end{aligned}
\tag{27}
$$

where $A_{sj} = g\alpha_{sj}$ is the normalized signal amplitude. The noise terms $\mathrm{d}W'_{s1}$ and $\mathrm{d}W'_{s2}$ are:

$$
\begin{aligned}
\mathrm{d}W'_{s1} &= \sqrt{\tfrac{\gamma_s}{\gamma'_s}}\mathrm{d}W_{s1}(\tau) + A_{s1}\mathrm{d}W_{p1}(\tau) + \sqrt{\xi}\mathrm{d}W_c(\tau), \\
\mathrm{d}W'_{s2} &= \sqrt{\tfrac{\gamma_s}{\gamma'_s}}\mathrm{d}W_{s2}(\tau) + A_{s2}\mathrm{d}W_{p2}(\tau) + \sqrt{\xi}\mathrm{d}W_c(\tau).
\end{aligned}
\tag{28}
$$

We can easily extend the above two CSDEs to the one-dimensional network consisting of N DOPOs with nearest neighbor coupling, as shown in Fig. 2. The CSDE of jth DOPO constructing such a one-dimensional DOPO network is

$$
\begin{aligned}
\mathrm{d}A_{sj} =& \left\{-A_{sj} + (p - A_{sj}^2)A_{sj}^* - \xi A_{sj-1} - \xi A_{sj+1}\right\}\mathrm{d}\tau + g\mathrm{d}W'_{sj} \\
\mathrm{d}W'_{sj} =& \sqrt{\frac{\gamma_s}{\gamma'_s}}\mathrm{d}W_{sj}(\tau) + A_{sj}\mathrm{d}W_{pj}(\tau) + \sqrt{\xi}\mathrm{d}W_{cj+1}(\tau) + \sqrt{\xi}\mathrm{d}W_{cj-1}(\tau).
\end{aligned}
\tag{29}
$$

It should be pointed out that the truncated Wigner CSDE is driven by the vacuum noise injected into the signal field $\mathrm{d}W_{sj}$, pump field $\mathrm{d}W_{pj}$ and injection path field $\mathrm{d}W_{cj}$ from external reservoirs, as shown by Eq.(28) or Eq.(29). On the other hand, the positive $P(\alpha, \beta)$ CSDE is driven only by the pump noise. This is because the coherent state basis sets for expanding the density operator in the positive $P(\alpha, \beta)$ theory carry the full vacuum fluctuation.

One last comment about the truncated Wigner theory, Eq.(29), is that the non-Gaussian nature of the DOPO signal field near the threshold is properly taken care of by this theory. Note that truncation of higher-order nonlinearities and neglect of non-Gaussian wavepacket tails are two different approximations.

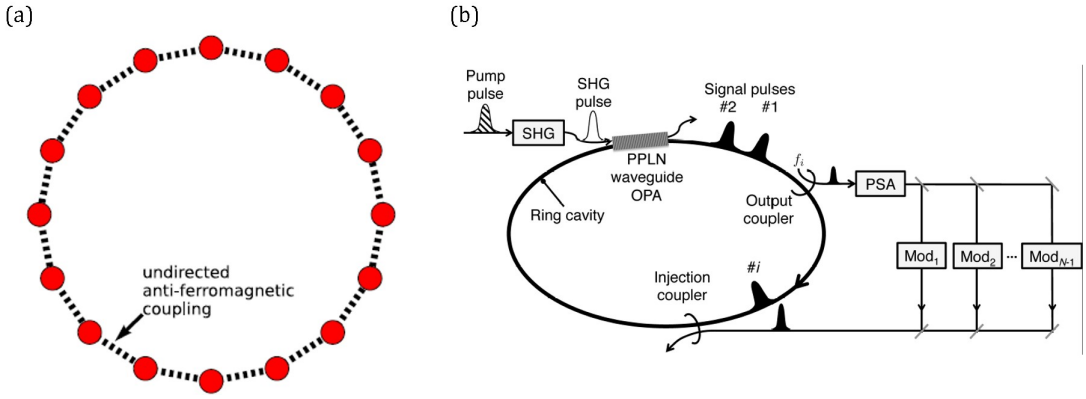

FIG. 2: (a) Sketch of one-dimensional network consisting of $N = 16$ DOPOs connected with nearest-neighbor identical anti-ferromagnetic couplings [5]. (b) A DOPO network with optical delay line coupling. The output coupler followed by the phase sensitive amplifier (DOPA: degenerate optical parametric amplifier) amplifies the in-phase amplitude $\hat{X}$ of each DOPO pulse, while the injection coupler combines the modulated feedback pulse with the target DOPO pulse, which implements the given Ising Hamiltonian. The state incident to the output coupler from an open port plays an important role in the behavior of this system [10].

3.4 Quantum entanglement and inseparability

The expectation value of a normally ordered operator is readily evaluated using the positive-P function [8].

$$\left\langle \hat{a}_{s1}^{\dagger j}\hat{a}_{s2}^{\dagger k}\hat{a}_{s1}^{l}\hat{a}_{s2}^{m}\right\rangle = \int \beta_{s1}^{j}\beta_{s2}^{k}\alpha_{s1}^{l}\alpha_{s2}^{m}P(\{\boldsymbol{\alpha}\},\{\boldsymbol{\beta}\})\mathrm{d}\boldsymbol{\alpha}\mathrm{d}\boldsymbol{\beta}, \tag{30}$$

while the expectation value of a symmetrically ordered operator is conveniently evaluated using the truncated Wigner function [9]:

$$\left\langle \hat{a}_{s1}^{\dagger j}\hat{a}_{s2}^{\dagger k}\hat{a}_{s1}^{l}\hat{a}_{s2}^{m}\right\rangle_{S} = \int \alpha_{s1}^{*j}\alpha_{s2}^{*k}\alpha_{s1}^{l}\alpha_{s2}^{m}W(\{\boldsymbol{\alpha}\})\mathrm{d}\boldsymbol{\alpha}. \tag{31}$$

Here, $\langle\cdots\rangle_S$ indicates the ensemble averaging after symmetrization of the operator inside the bracket. The normalized correlation functions between the two DOPOs (Fig. 1) for the in-phase amplitude $\hat{x} = (\hat{a} + \hat{a}^\dagger)/2$ and quadrature-phase amplitude $\hat{p} = (\hat{a} - \hat{a}^\dagger)/(2i)$ are defined as

$$\begin{aligned} \mathrm{C}(\hat{x}_{s1},\hat{x}_{s2}) &= \frac{\langle \hat{x}_{s1}\hat{x}_{s2}\rangle}{\langle \Delta x_{s1}\Delta x_{s2}\rangle} = \frac{\langle c_{s1}c_{s2}\rangle}{\sqrt{\left\langle c_{s1}^2\right\rangle - \langle c_{s1}\rangle^2}\sqrt{\left\langle c_{s2}^2\right\rangle - \langle c_{s2}\rangle^2}} \\ \mathrm{C}(\hat{p}_{s1},\hat{p}_{s2}) &= \frac{\langle \hat{p}_{s1}\hat{p}_{s2}\rangle}{\langle \Delta p_{s1}\Delta p_{s2}\rangle} = \frac{\langle s_{s1}s_{s2}\rangle}{\sqrt{\left\langle s_{s1}^2\right\rangle - \langle s_{s1}\rangle^2}\sqrt{\left\langle s_{s2}^2\right\rangle - \langle s_{s2}\rangle^2}}, \end{aligned} \tag{32}$$

where $c_X = (\alpha_X + \alpha_X^*)/2$, $s_X = (\alpha_X - \alpha_X^*)/(2i)$, and $\Delta O = \sqrt{\left\langle \hat{O}^2\right\rangle - \left\langle \hat{O}\right\rangle^2}$.

We can define the EPR-like operators by $\hat{u}_+ = \hat{x}_{s1} + \hat{x}_{s2}$ and $\hat{v}_- = \hat{p}_{s1} - \hat{p}_{s2}$ to evaluate the degree of negative and positive quantum correlation. We assumed that the two DOPOs are coupled with the anti-ferromagnetic interaction, i.e. $e^{ik_c z} = e^{-ik_c z} = -1$, so that we expect that $\hat{x}_{s1}$ and $\hat{x}_{s2}$ are negatively correlated, while $\hat{p}_{s1}$ and $\hat{p}_{s2}$ are positively correlated. The condition for negative (or positive) quantum correlation is given by $\left\langle \Delta\hat{u}_+^2\right\rangle < 0.5$, or $\left\langle \Delta\hat{v}_-^2\right\rangle < 0.5$, while the criterion for entanglement (inseparability) is given by $\left\langle \Delta\hat{u}_+^2\right\rangle + \left\langle \Delta\hat{v}_-^2\right\rangle < 1$ [11]. Figure 3 compares the total variances of the EPR-like operator, computed by the positive-P representation and by the truncated Wigner representation [5]. Here, the pump rate is linearly increased from zero to 1.5 times the oscillation threshold over time $\tau = 200$, i.e. $p = 1.5\ (\tau/200)$. The saturation parameter is $g = 0.01$. As can be seen in Fig. 3, the two coupled DOPOs feature inseparability, i.e., $\left\langle \Delta\hat{u}_+^2\right\rangle + \left\langle \Delta\hat{v}_-^2\right\rangle \leqslant 1$, when the system evolves from below to above the oscillation threshold. Note that the coupled DOPO threshold pump rate is $p_{th} = 1 - \xi$ rather than $p_{th}^{(0)} = 1$ for a solitary (uncoupled) DOPO [12]. Increasing the coupling constant ξ enhances the inseparability. The results obtained using the positive-P representation are indistinguishable from those by the truncated Wigner representation. Our numerical simulation confirms that the difference in the total variances, $\left\langle \Delta\hat{u}_+^2\right\rangle + \left\langle \Delta\hat{v}_-^2\right\rangle$, evaluated using the positive-P representation and the truncated Wigner representation is within the statistical error due to the finite number of samples $M = 200,000$, which is shown only in Fig. 3(a) as vertical bars.

In the one-dimensional network shown in Fig. 2(a), we can define the EPR-like operators $\hat{u}_{1D}$ and $\hat{v}_{1D}$ if the number N of DOPOs is even:

$$\hat{u}_{1D} = \sum_{j=1}^{N} \hat{x}_{sj}, \hat{v}_{1D} = \sum_{j=1}^{N} (-1)^j \hat{p}_{sj}. \tag{33}$$

We made a proof in the Appendix that the operator $\hat{u}_{1D}$ and $\hat{v}_{1D}$ are the indicators of the quantum correlation and inseparability of the system.

Figure 4 shows the total variance of the EPR-like operator $\hat{u}_{1D} + \hat{v}_{1D}$ when we inject the

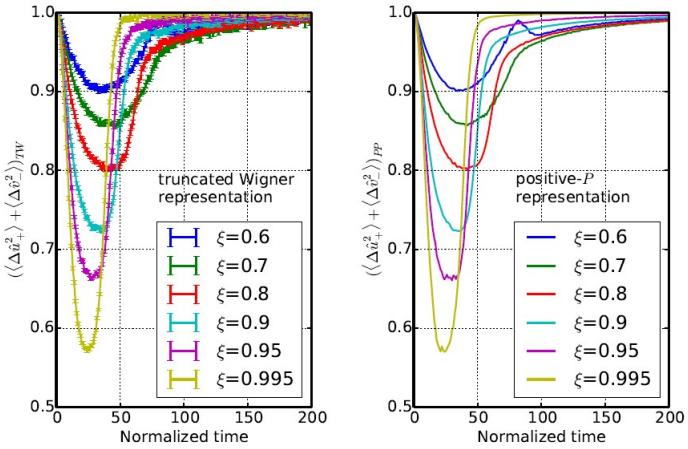

FIG. 3: Total variance of the EPR-like operator $\hat{u}_+ + \hat{v}_-$ calculated by the truncated Wigner representation (left panel (a)) and positive-P representation (right panel (b)). The statistical error bars due to the finite number of samples $M = 200.000$ are only plotted in Fig. 3(a) [5].

squeezed vacuum state with reduced quantum noise, $e^{-2r}/4$, in the in-phase amplitude and enhanced quantum noise, $e^{2r}/4$, in the quadrature-phase amplitude with r the squeezing parameter into the open port of the output coupler (Fig. 2(b)) in the $N = 16$ one-dimensional DOPO network [5]. Here, the pump rate gradually increases from zero to 0.375 times the oscillation threshold over time $\tau = 200$, i.e. $p = 0.375\ (\tau/200)$. The saturation parameter is $g = 0.01$ and the coupling constant $\xi = 0.4$. If a standard vacuum fluctuation ($r = 0$) is incident on the output coupler, the quantum correlation exists in the quadrature-phase amplitude ($\langle \Delta \hat{v}_{1D}^2 \rangle < N/4$) but only classical correlation exists in the in-phase amplitude ($\langle \Delta \hat{u}_{1D}^2 \rangle \geqslant N/4$) [5]. On the other hand, if we inject squeezed vacuum states ($r > 0$), the quantum correlation exists in both in-phase and quadrature-phase amplitudes. Note that the variance of $\hat{u}_{1D} + \hat{v}_{1D}$ is below the standard quantum limit ($N/2 = 8$), which is the criterion of inseparability and holds even without a squeezed input state.

In Fig. 3, we assume relatively large coupling constants $\xi\ (= 0.4 - 0.995)$. Such a strong coupling is not unrealistic if we amplify the out-coupled field with a noiseless phase sensitive amplifier (PSA) as shown in Fig. 2(b).

3.5 Quantum discord

The quantum correlation is the general property of a composite quantum system in which a local measurement performed on a sub-system changes the state of the whole system. There

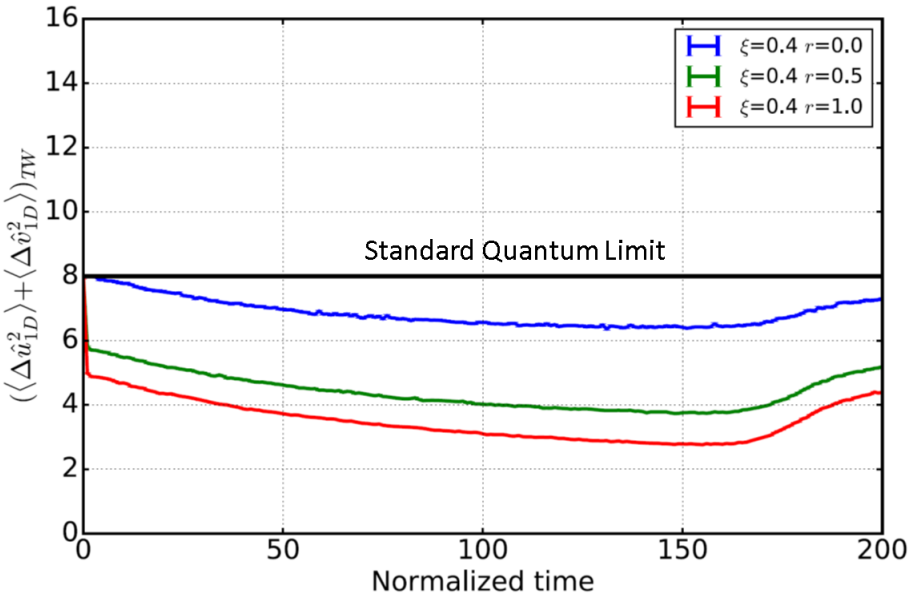

FIG. 4: The variance of $\hat{u}_{1D} + \hat{v}_{1D}$ versus normalized time τ for various squeezing parameters r. $r = 0$ corresponds to the normal vaccum state input to the output coupler [5].

is a weaker but broader definition of quantum correlation than the widely used measure of entanglement, showing that even separable states can have important quantum features.

Quantum discord [13] is a measure of the quantum correlation of a composite system, based on two different definitions of the mutual information of a bipartite system. Suppose we have a bipartite system AB composed of partial systems A and B. The mutual information based on the total and sub-system entropy is

$$I(\hat{\rho}_{AB}) = S(\hat{\rho}_A) + S(\hat{\rho}_B) - S(\hat{\rho}_{AB}), \tag{34}$$

where $S(\hat{\rho}) = -\mathrm{Tr}\,(\hat{\rho}\log\hat{\rho})$ is the von Neumann entropy. $\hat{\rho}_A = \mathrm{Tr}_B(\hat{\rho}_{AB})$ and $\hat{\rho}_B = \mathrm{Tr}_A(\hat{\rho}_{AB})$ are the entropies associated with the reduced density operators for the sub-systems A and B. Alternatively, the mutual information can be defined using the conditional entropy $S(A|B)$, which varies with the measurement basis for the sub-system B, because each local measurement can perturb the total system in a different way. To evaluate the genuine quantum correlation, the measurement basis which disturbs the total system least must be chosen. The mutual information based on the conditional entropy is defined as

$$J^{\leftarrow}(\hat{\rho}_{AB}) = S(\hat{\rho}_A) - \inf_{\Pi_i^B} \sum_i p_i S(\hat{\rho}_{A|i}), \tag{35}$$

where i is the index for the components of the positive operator-valued measure (POVM) measurement basis $\{\Pi_i^B\}$ for the sub-system B. The POVM measurement means an exact measurement performed for Hermitian operators, the detail of which will be discussed in next Chapter. $\hat{\rho}_{A|i}$ is the post-measurement state of the sub-system A provided that the ith state is measured in the sub-system B and p_i is the probability for obtaining the $i-$th state. $\inf\left(\pi_i^B\right)$ means the optimization of the POVM measurements $\left(\pi_i^B\right)$ to perturb the system least. The quantum discord is defined as the difference of the above two mutual information [13]:

$$D^{\leftarrow}(\hat{\rho}_{AB}) = I(\hat{\rho}_{AB}) - J^{\leftarrow}(\hat{\rho}_{AB}). \tag{36}$$

In general, system without entanglement can have nonzero discord, and it has been reported that such a state may be useful for a nontrivial quantum speedup in certain problems [14, 15].

The optimization of the measurement basis in Eq.(35) is generally hard. However, for the case of Gaussian states and local measurement limited to Gaussian POVMs, the analytic formulas for the quantum discord have been derived [16, 17] . They quantify the amount of genuine quantum correlation for a large part of Gaussian states, including two-mode squeezed states, coherent states, and the vacuum state [17]. We now estimate the discord of our system using the *Gaussian quantum discord*. Here, we consider the unnormalized quadrature amplitudes for the two DOPOs $[\hat{r}] = 2\,[\hat{x}_1, \hat{p}_1, \hat{x}_2, \hat{p}_2]$. Then, a two-mode Gaussian state is characterized with the covariance matrix of them:

$$\boldsymbol{\sigma}_G = \left[\frac{1}{2}\langle \hat{r}_j\hat{r}_k + \hat{r}_k\hat{r}_j\rangle - \langle \hat{r}_j\rangle\langle \hat{r}_k\rangle\right] = \begin{pmatrix} \boldsymbol{\alpha}_M & \boldsymbol{\gamma}_M \\ \boldsymbol{\gamma}_M^{\mathrm{T}} & \boldsymbol{\beta}_M \end{pmatrix}, \tag{37}$$

where $\boldsymbol{\alpha}_M$, $\boldsymbol{\beta}_M$ and $\boldsymbol{\gamma}_M$ are 2×2 matrices. The state can be equivalently characterized by the quantities called *symplectic invariants* defined as

$$A_S = \det\boldsymbol{\alpha}_M,\ B_S = \det\boldsymbol{\beta}_M,\ C_S = \det\boldsymbol{\gamma}_M,\ D_S = \det\boldsymbol{\sigma}_G. \tag{38}$$

When we write the binary entropy function as $f_B(X) = (X + 1/2)\log(X + 1/2) - (X - 1/2)\log(X - 1/2)$, and the quantities called *symplectic eigenvalues* as $\nu_{\pm}^2 = 1/2\left(\Delta \pm \sqrt{\Delta^2 - 4D_S}\right)$, $\Delta = A_S + B_S + 2C_S$, the Gaussian quantum discord is given by

$$D^{\leftarrow}(\sigma_G) = f_B\left(\sqrt{B_S}\right) - f_B(\nu_-) - f_B(\nu_+) + \inf_{\boldsymbol{\sigma}_0} f_B\left(\sqrt{\det \boldsymbol{\epsilon}}\right). \tag{39}$$

Here, $\boldsymbol{\sigma}_0$ is the Gaussian measurement basis for the partial system B. $\boldsymbol{\epsilon}$ is the covariance matrix for the partial system A after B has been locally measured. The last term in Eq. (39) can be optimized analytically within the range of Gaussian POVMs (adding Gaussian ancilla bits, symplectic transformations and a homodyne detection), yielding [18].

$$\begin{aligned}\inf_{\boldsymbol{\sigma}_0} \det \boldsymbol{\epsilon} =& \frac{2C_S^2 + (B_S-1)(D_S-A_S) + 2|C_S|\sqrt{C_S^2 + (B_S-1)(D_S-A_S)}}{(-1+B_S)^2}, \\ & \text{if } (D_S - A_S B_S) \leqslant (1+B_S) C_S^2 (A_S + D_S), \\ =& \frac{A_S B_S - C_S^2 + D_S - \sqrt{C_S^4 + (D_S-A_S)^2 - 2C_S^2(A_S B_S + D_S)}}{2B_S}, \text{ otherwise.}\end{aligned} \tag{40}$$

In addition, a simpler formula for two-mode squeezed states (including squeezed vacuum states) has been also derived as [16].

$$\sqrt{\det \boldsymbol{\epsilon}} = \frac{\sqrt{A_S} + 2\sqrt{A_S B_S} + 2C_S}{1+\sqrt{B_S}}. \tag{41}$$

A bipartite state with $D^{\leftarrow}(\boldsymbol{\sigma}_G) \geqslant 1$ always has the entanglement between its elements. A certain entangled state can also have a value of the quantum discord smaller than 1 [16].

Figure 5 shows the quantum discord when the DOPO state is approximated as a Gaussian state [4]. It basically reflects the quantum correlation formed in $\hat{p}_1$ and $\hat{p}_2$. When $\hat{p}_1$ and $\hat{p}_2$ are squeezed and have positive correlation, the system holds a relatively large discord. Moreover, a finite value $D^{\leftarrow} \sim 0.02$ is observed at pump rates well above threshold. It is worth noting that this finite discord is not attributed to the squeezing in the DOPOs as previously discussed [16], but the mixture of coherent states with classical correlation can have this finite value of discord. We have found that the variances in $\hat{x}_j$ and $\hat{p}_j$ quickly verge on 1/4 after the oscillation threshold is passed, thus the states are well described as coherent states. Also, the curves with the finite discord is associated with an almost perfect correlation of x such as $\langle \hat{x}_1 \hat{x}_2 \rangle = -0.9999 \sim -1.0000$. On the other hand, significant intra-cavity signal field dissipation can cancel out the discord at well above the oscillation threshold, as shown in Fig. 5 [4].

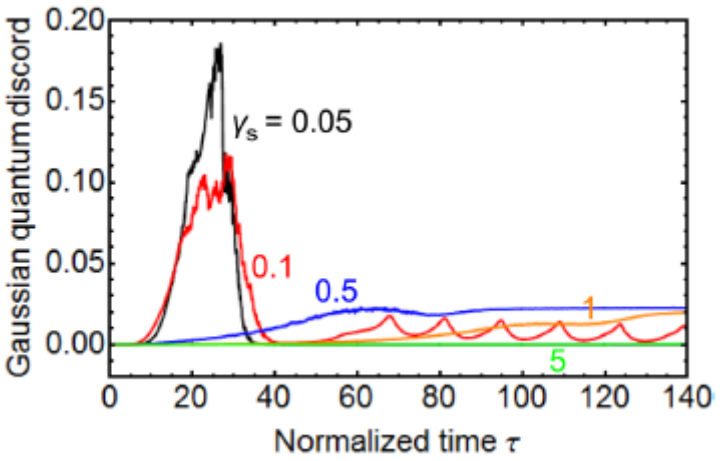

FIG. 5: (Color online) Quantum discord when the DOPO state is approximated as a bipartite Gaussian state. Squeezing in the DOPOs near the threshold and the mutual injection gives a large discord when α_s is samll. Coherent fields at well above the threshold and coherent communication lead to a finite discord of ~ 0.02. 50000 stochastic runs for each curve [4].

The particular states of the two DOPOs at well above the threshold with out-of-phase correlation between $\hat{x}_1$ and $\hat{x}_2$ have the covariance matrix given by

$$\hat{\rho}_{cl} = \frac{1}{2} |\alpha_{cl}\rangle_1 |-\alpha_{cl}\rangle_{2\,2} \langle -\alpha_{cl}|_1 \langle \alpha_{cl}| + \frac{1}{2} |-\alpha_{cl}\rangle_1 |\alpha_{cl}\rangle_{2\,2} \langle \alpha_{cl}|_1 \langle -\alpha_{cl}| \,, \tag{42}$$

$$\sigma(\hat{\rho}_{cl}) = \begin{pmatrix} 4\alpha_{cl}^2 + 1 & 0 & -4\alpha_{cl}^2 & 0 \\ 0 & 1 & 0 & 0 \\ -4\alpha_{cl}^2 & 0 & 4\alpha_{cl}^2 + 1 & 0 \\ 0 & 0 & 0 & 1 \end{pmatrix}, \tag{43}$$

where α_{cl} is the real and positive amplitude of the coherent states in the DOPOs. We have found that the Gaussian discord calculated with Eq.(43) verges on $D^{\leftarrow} \sim 0.02356$ for $\alpha_{cl} \gtrsim 50$, which is in a good agreement with the values in the simulation results shown in Fig. 5. Equation (42) represents a mixture of two Gaussian states, so that the result indicates a genuine quantum correlation exists in the two coherent states with the correlation between their eigenvalues.

3.6 Summary

Some of the important conclusions of Chapter III are summarized below.

1. The c-number stochastic differential equations (CSDE) based on the positive $P(\alpha, \beta)$ representation are given by Eqs.(23) and (24).

2. The CSDE based on the truncated Wigner $W(\alpha)$ representation are given by Eq.(27) for two coupled DOPOs and by Eq.(29) for N DOPOs in one dimensional ring.

3. An EPR-like operator, Eq.(33), can be defined to numerically test the inseparability and entanglement of coupled DOPOs.

4. The simple optical delay line coupling QNN in one-dimensional network with nearest-neighbor anti-ferromagnetic coupling is shown to possess the inseparability and entanglement for a wide range of pumping rates as shown in Fig. 3 and Fig. 4.

5. Quantum correlation in a composite quantum system can be evaluated by alternative measure, quantum discord, defined by Eq.(36) for general case or Eq.(39) for Gaussian states.

6. The optical delay line coupling QNN shows the strong quantum discord near the threshold and supports a small quantum discord of $D \sim 0.02$ even at well above the threshold.

Appendix: Properties of the EPR-like operators

Theorem 1. *If the system is separable, the inequality* $\langle \Delta \hat{u}_{1D}^2 \rangle + \langle \Delta \hat{v}_{1D}^2 \rangle \geqslant N/2$ *is satisfied.*

Proof. The left-hand side of inequaity, $\langle \Delta \hat{u}_{1D}^2 \rangle + \langle \Delta \hat{v}_{1D}^2 \rangle$, can be written as

$$\left\langle \Delta \hat{u}_{1D}^2 \right\rangle + \left\langle \Delta \hat{v}_{1D}^2 \right\rangle = \mathrm{Tr}[\hat{\rho} \hat{u}_{1D}^2] - (\mathrm{Tr}[\hat{\rho} \hat{u}_{1D}])^2 + \mathrm{Tr}[\hat{\rho} \hat{v}_{1D}^2] - (\mathrm{Tr}[\hat{\rho} \hat{v}_{1D}])^2. \tag{44}$$

If the system is separable, the system density operator $\hat{\rho}$ can be decomposed as the tensor product of the density operator of each DOPO $\hat{\rho}_{jk}$, i.e.

$$\hat{\rho} = \sum_k q_k \hat{\rho}_{1k} \otimes \hat{\rho}_{2k} \otimes \cdots \otimes \hat{\rho}_{Nk} = \sum_k q_k \prod_{j=1}^{N} \hat{\rho}_{jk}. \tag{45}$$

Here q_k is the mixing probability of each tensor product $\prod_{j=1}^{N}\hat{\rho}_{jk}$ and $\sum_k q_k = 1$. Each term of Eq.(44) can be written as

$$\begin{aligned}
\mathrm{Tr}[\hat{\rho}\hat{u}_{1D}^2] =& \mathrm{Tr}\left[\sum_{\mathrm{k}} \mathrm{q_k} \prod_{\mathrm{j=1}}^{\mathrm{N}} \hat{\rho}_{\mathrm{jk}} \hat{\mathrm{u}}_{\mathrm{1D}}^2\right] \\
=& \mathrm{Tr}\left[\sum_{\mathrm{k}} \mathrm{q_k} \prod_{\mathrm{j=1}}^{\mathrm{N}} \hat{\rho}_{\mathrm{jk}} \sum_{\mathrm{j=1}}^{\mathrm{N}} (\hat{\mathrm{x}}_{\mathrm{sj}}^2 + 2 \sum_{\mathrm{l=j+1}}^{\mathrm{N}} \hat{\mathrm{x}}_{\mathrm{sj}} \hat{\mathrm{x}}_{\mathrm{sl}})\right] \\
=& \sum_k q_k \sum_{j=1}^{N} \left\{ \left\langle \hat{x}_{sj}^2 \right\rangle_k + 2 \sum_{l=j+1}^{N} \left\langle \hat{x}_{sj} \right\rangle_k \left\langle \hat{x}_{sl} \right\rangle_k \right\} \\
=& \sum_k q_k \sum_{j=1}^{N} \left\{ \left\langle \Delta\hat{x}_{sj}^2 \right\rangle_k + \left\langle \hat{x}_{sj} \right\rangle_k^2 + 2 \sum_{l=j+1}^{N} \left\langle \hat{x}_{sj} \right\rangle_k \left\langle \hat{x}_{sl} \right\rangle_k \right\} \\
=& \sum_k q_k \sum_{j=1}^{N} \left\langle \Delta\hat{x}_{sj}^2 \right\rangle_k + \sum_k q_k \left\langle \hat{u}_{1D} \right\rangle_k^2 ,
\end{aligned} \tag{46}$$

$$\left(\mathrm{Tr}\left[\hat{\rho}\hat{\mathrm{u}}_{\mathrm{1D}}\right]\right)^2 = \left(\mathrm{Tr}\left[\sum_k q_k \prod_{j=1}^{N} \hat{\rho}_{jk} \hat{u}_{1D}\right]\right)^2 = \left(\sum_k q_k \left\langle \hat{u}_{1D} \right\rangle_k\right)^2 , \tag{47}$$

$$\begin{aligned}
\mathrm{Tr}\left[\hat{\rho}\nu_{\mathrm{1D}}^2\right] =& \mathrm{Tr}\left[\sum_{\mathrm{k}} \mathrm{q_k} \prod_{\mathrm{j=1}}^{\mathrm{N}} \hat{\rho}_{\mathrm{jk}} \hat{v}_{\mathrm{1D}}^2\right] = \mathrm{Tr}\left[\sum_{\mathrm{k}} \mathrm{q_k} \prod_{\mathrm{j=1}}^{N} \hat{\rho}_{\mathrm{jk}} \times \sum_{\mathrm{j=1}}^{N} \left(\hat{\mathrm{p}}_{\mathrm{sj}}^2 + 2 \sum_{\mathrm{l=j+1}}^{N} (-1)^{\mathrm{j+l-2}} \hat{\mathrm{p}}_{\mathrm{sj}} \hat{\mathrm{p}}_{\mathrm{sl}}\right)\right] \\
=& \sum_k q_k \sum_{j=1}^{N} \left\{ \left\langle \hat{p}_{sj}^2 \right\rangle_k + 2 \sum_{l=j+1}^{N} (-1)^{j+l-2} \left\langle \hat{p}_{sj} \right\rangle_k \left\langle \hat{p}_{sl} \right\rangle_k \right\} \\
=& \sum_k q_k \sum_{j=1}^{N} \left\{ \left\langle \Delta\hat{p}_{sj}^2 \right\rangle_k + \left\langle \hat{p}_{sj} \right\rangle_k^2 + 2 \sum_{l=j+1}^{N} (-1)^{j+l-2} \left\langle \hat{p}_{sj} \right\rangle_k \left\langle \hat{p}_{sl} \right\rangle_k \right\} \\
=& \sum_k q_k \sum_{j=1}^{N} \left\langle \Delta\hat{p}_{sj}^2 \right\rangle_k + \sum_k q_k \left\langle \hat{v}_{1D} \right\rangle_k^2 ,
\end{aligned} \tag{48}$$

$$\begin{aligned}
\left(\mathrm{Tr}\left[\hat{\rho}\hat{v}_{1D}\right]\right)^2 &= \left(\mathrm{Tr}\left[\sum_k q_k \prod_{j=1}^{N} \hat{\rho}_{jk} \hat{v}_{1D}\right]\right)^2 \\
&= \left(\sum_k q_k \left\langle \hat{v}_{1D} \right\rangle_k\right)^2 .
\end{aligned} \tag{49}$$

Now we use the inequalities $\sum_k q_k \left\langle \hat{u}_{1D} \right\rangle_k^2 = \sum_k q_k \sum_k q_k \left\langle \hat{u}_{1D} \right\rangle_k^2 \geqslant \left(\sum_k q_k \left\langle \hat{u}_{1D} \right\rangle_k\right)^2$ and

$\sum_k q_k \langle \hat{v}_{1D} \rangle_k^2 = \sum_k q_k \sum_k q_k \langle \hat{v}_{1D} \rangle_k^2 \geqslant (\sum q_k \langle \hat{v}_{1D} \rangle_k)^2$, which are derived from Cauthy-Schwarz inequality. Moreover, $\sum_k q_k \left(\langle \Delta \hat{x}_{sj}^2 \rangle_k + \langle \Delta \hat{p}_{sj}^2 \rangle_k \right) \geqslant 0.5$ is derived from the uncertainty principle. We can conclude that the inequality $\langle \Delta \hat{u}_{1D}^2 \rangle + \langle \Delta \hat{v}_{1D}^2 \rangle \geqslant N/2$ is satisfied if the state is separable.

Theorem 2. *If the inequalities* $\langle \Delta \hat{u}_{1D}^2 \rangle + \langle \Delta \hat{v}_{1D}^2 \rangle < N/2$ *is satisfied, the system is inseparable and the quantum entanglement exists.*

Proof. It is the contraposition of Theorem 1.

---

[1] A. Marandi et al., Nature Photonics 8, 937 (2014).

[2] K. Takata et al., Sci. Rep. 6, 34089 (2016).

[3] T. Inagaki et al., Nature Photonics 10, 415 (2016).

[4] K. Takata et al., Phys. Rev. A 92, 043821 (2015).

[5] D. Maruo et al., Phys. Scr. 91, 083010 (2016).

[6] H. J. Carmichael, Statistical Methods in Quantum Optics 1: Master Equations and Fokker-Planck Equations (Springer-Verlag Berlin Heidelberg, 2002).

[7] R. J. Glauber, Phys. Rev. 131, 2766 (1963).

[8] P. D. Drummond and C. W. Gardiner, J. Phys. A 13, 2353 (1980).

[9] D. F. Walls and G. J. Milburn, Quantum Optics (Springer, Berlin-Heisengerg, 2007).

[10] Y. Haribara et al., Entropy 18, 151 (2016).

[11] L-M. Duan et al., Phys. Rev. Lett. 84, 2722 (2000).

[12] Z. Wang et al., Phys Rev. A 88, 063853 (2013).

[13] H. Ollivier and W. H. Zurek, Phys. Rev. Lett. 88, 017901 (2001).

[14] B. P. Lanyon et al., Phys. Rev. Lett. 101, 200501 (2008).

[15] E. Knill and R. Laflamme, Phys. Rev. Lett. 81, 5672 (1998).

[16] P. Giorda and M. G. A. Paris, Phys. Rev. Lett. 105, 020503 (2010).

[17] G. Adesso and A. Datta, Phys. Rev. Lett. 105, 030501 (2010).

[18] S. Pirandola at el., Phys. Rev. Lett. 113, 140405 (2014).

Written by Y. Yamamoto, K. Takata, and D. Maruo

version 1